

R. V. Vasil'eva, A. D. Zuev,  
V. L. Moshkov, L. G. Tkhorik,  
and V. A. Shingarkina

UDC 532.517.4.532.593

The phenomenon of turbulent mixing of gases on contact surfaces is found in many gas dynamic problems and devices, for example, in shock [3] and electrical discharge [4] tubes, and in cylindrical and spherical explosion. Development of turbulent mixing in these devices is essentially caused by Rayleigh-Taylor instability is presented for the isothermal case in [6], while it was extended to the nonisothermal case in [7].

In contrast to other devices, in a shock tube as initial turbulence exists, caused by rupture of the diaphragm. A number of studies have considered the process of rupture and shock wave formation [8-13]. However, questions concerning formation of a contact region in the process of wave motion away from the diaphragm and its effect on parameters of the shock compressed gas remain unclarified. This is a complex physical problem and requires the use of special methods for measurement of particle concentration, since well developed interferometric methods cannot be used in turbulized flows, and moreover, they cannot distinguish the individual components in the mixture of driver and driven gases. Optical methods have only established that a turbulent flow region follows behind the hot charge of shock-compressed gas. Therefore, in practical shock tube applications the concept of a contact region has been introduced in place of the contact surface. Until the present the question of the stability of the boundaries of this region has not been considered, and there has been practically no discussion of mixing of driver and driven gases in this region in the literature. The length of the driver and driven gas mixing zone in a shock tube at a fixed distance from the diaphragm was first established in [14] using absorption of IR radiation in CO<sub>2</sub> molecules, while the distribution of mean density of the driven gas in the mixing region was obtained in [15] using absorption of soft x radiation, with the driven gas being a heavy inert gas and the driver a light gas. However, the dynamics of the process were not considered in that study.

The present study will investigate the development of a turbulent mixing zone as it moves along the shock tube far from the diaphragm.

The experiments were performed in a conventional diaphragm-type shock tube. Aluminum diaphragms were used, which were opened under pressure either with an X-shaped cutter or no cutter. Diaphragm thicknesses of 0.45 and 0.35 mm were used. The inner diameter of the low pressure channel was 50 mm, with a length of 5 m. The high pressure chamber was 1 m long. The driver gas used was xenon at initial pressures of 0.67-13.3 kPa.

Figure 1 shows the measurement section and equipment. The pressure behind the shock wave front and the shock wave front velocity were measured by piezosensors 1. The radiation produced by the shock-heated gas was measured with photomultiplier 2 and light guide 3. Gas density was measured from absorption of soft x rays [15]. In the majority of the experiments all sensors and windows were mounted flush with the tube walls. To measure density in the flow core, special inserts were made with an aerodynamic outer section and extending 1 cm into the flow. The insert thickness at the midpoint was 5 mm, diameter of the inner viewing orifice was 2 mm, and a beryllium window 4 for x-ray passage was mounted on the face. The location of the inserts is shown by dashed lines. Measurements were performed in three tube sections at 15, 50, and 92 diameters from the diaphragm. A nonstandard tube at a voltage of 11.5 kV was used for the x-ray source. An FEU-144 photomultiplier with NaI scintillator was used as the x-ray detector. The experiments recorded the intensity of the incident x radiation  $I_0$  and the intensity after passage through the absorbing layer  $I$ . For monochromatic x radiation

$$I/I_0 = \exp\left(-\mu \int_0^h \rho(y) dy\right).$$

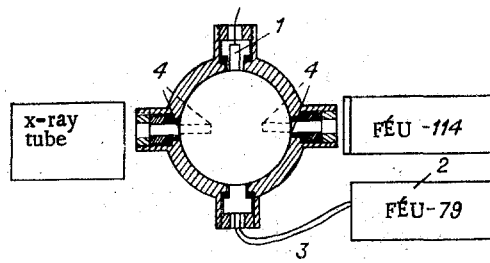


Fig. 1

The ray was directed along the y axis across the shock tube;  $h$  is the thickness of the absorbing layer;  $\rho(y)$  is the density distribution;  $\mu$  is the absorption coefficient, which depends intensely on the atomic number of the element ( $\mu \sim z^4$ );  $\mu$  is determined during calibration of the measurement system. System calibration was performed with the low pressure chamber statically filled with the gas to be studied. Thus the ratio  $I/I_0$  directly determines the total mass of gas included in the absorbing layer bounded by the beam width of 2 mm. For a homogeneous density distribution across the tube this value can be used to determine the true density of the gas, while for an inhomogeneous distribution we can characterize a mean density

$$\langle \rho \rangle = \frac{1}{h} \int_0^h \rho(y) dy.$$

The intense dependence of the x-ray absorption coefficient on atomic

number of the element permits reliable separation of the regions containing driver and driven gases. To this end, the following pairs of driven and driver gases were used: a) xenon-helium (absorption caused by Xe, no absorption in driver gas); 2) air mixture of (98.8%  $H_2$  + 1.2% Xe) (absorption caused by Xe component in driver gas absorption in air negligibly small); 3) xenon mixture of (98.8%  $H_2$  + 1.2% Xe) (absorption in driven and driver gases caused by Xe).

The experimental technique used permitted determination of the distribution of both driven and driver gases in the turbulent contact region, evaluation of the homogeneity of this region across the shock tube, and tracking of the development of the turbulent contact region as it moves along the shock tube.

The oscillograms shown in Fig. 2 illustrate the main features of the experiment. Shown are x-ray signals 1 and intrinsic radiation from the shock-compressed gas charge 2 in the sections  $X = 15d$  (A) and  $92d$  (B) for various experimental conditions: a) Xe-He,  $p_0 = 1.7$  kPa,  $M_0 = 9$ , without inserts; b) Xe-He,  $p_0 = 1.7$  kPa,  $M_0 = 9$ , with inserts; c) Xe-( $H_2$  + Xe) mixture,  $p_0 = 1.7$  kPa,  $m_0 = 9$ , without inserts; d) air-( $H_2$  + Xe) mixture,  $p_0 = 1.7$  kPa,  $M_0 = 5$ , without inserts; arrows indicate position of shock wave fronts. Before arrival of the shock wave there is a negative polarity x-ray signals, attenuated as compared to the signal in vacuum by the amount of xenon absorption in the low pressure chamber. Arrival of the shock wave is characterized by a change in the x-ray signal, corresponding to the increase in density in the shock wave front. Intrinsic radiation from the plasma appears simultaneously. From this point the absorption of the x-ray signal is determined by the density distribution in the shock-compressed gas charge (region 1, Fig. 2A, a). The end of the hot charge corresponds to an increase in x-ray signal (Fig. 2a, b) and termination of the plasma radiation. There follows a contact mixing region (region 2, Fig. 2A, a), the length of which is comparable to the length of the hot charge. If helium is used as the driver gas, after the contact region passes, the x-ray signal approaches its value in a vacuum  $I_0$ . When the mixture  $H_2$  + Xe is used as a driver, absorption in the Xe component of the driver is close to that in the shock-compressed gas charge (Fig. 2c). The distribution of the driver gas in the contact region can be interpreted easily if a gas which absorbs x rays very weakly, like air, is used for the driven gas (Fig. 2d). It is evident from Fig. 2d that the region of penetration of the driver gas into the driven increases with motion along the tube.

Figure 3 shows mean density distributions for the driven gas 1 and density in the flow core 2 for various distances from the diaphragm: a)  $X = 15d$ ; b)  $X = 92d$ . The dash-dot lines denote the leading and trailing boundaries of the contact mixing regions. Upon transition from

the time intervals measured in experiment to spatial  $\left( x = \int_0^t u_c dt \right)$  it is necessary to know the velocity of the companion flow  $u_c$  in the measurement section. Measurements of flow velocity in the shock-compressed gas charge performed in [16; 17] have shown that in a real shock tube in a fixed section the velocity of the companion flow increases along the charge. The velocity

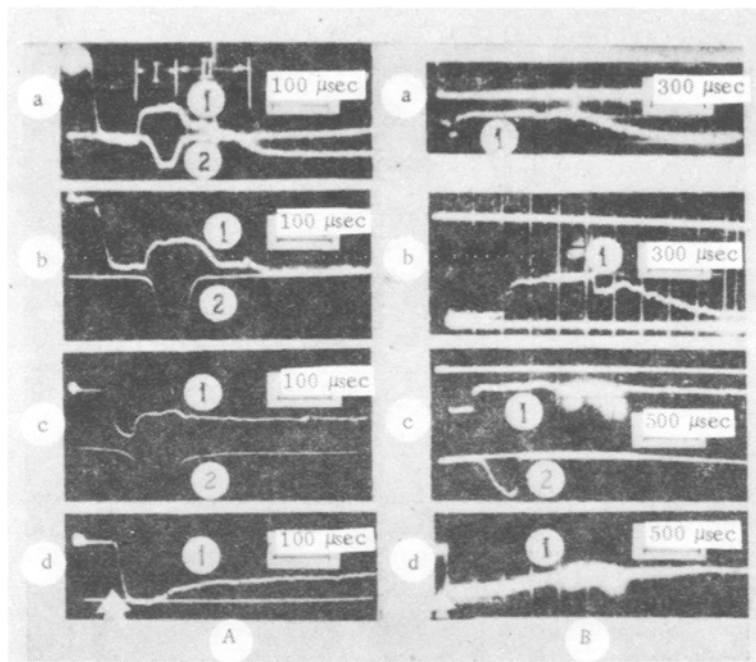


Fig. 2

of the shock front also changes, however measurements have shown that upon transition from  $X = 50d$  to  $X = 92d$  the front velocity falls by less than 2%. Consequently, it can be assumed that the front velocity  $u_s = \text{const}$ . Then in the first approximation, neglecting gas flow through the boundary layer, the increase in velocity of the comparison flow can be estimated from the condition  $\langle \rho \rangle (u_s - u_c) = \text{const}$ , where  $\langle \rho \rangle$ ,  $u_s$  are experimentally determined. The velocity in the contact mixing region and in the driver gas are taken equal to the velocity of the driven gas at the leading boundary of the contact region. Estimates performed indicate that uncertainty in determining spatial coordinates does not exceed 10%.

In Fig. 3 the numeral I denotes the shock-compressed charge, and II is the contact mixing region. The end of the charge and beginning of the contact mixing region were determined from the termination of driven gas scintillation and the abrupt change in the derivative  $\partial \langle \rho \rangle / \partial x$ . It was assumed that the end of the mixing zone is located where the x-ray signal rises to 0.9 times its value in a vacuum. For the signal in vacuum  $I_c$  we may use the x-ray signal in the helium driver gas region.

The degree of flow homogeneity across the tube can be evaluated by comparing results of measurements made with the inserts ( $h = 3 \text{ cm}$ ) and without them ( $h = 5 \text{ cm}$ ). The effects of the inserts on the results of measurements in the flow core can be determined by analysis of density measurements in the shock-compressed gas charge, where the density distribution across the charge is relatively homogeneous. The increase along the probe is caused by energy losses to ionization, radiant cooling, the effect of the boundary layer, and heat losses due to electronic thermal conductivity [3]. It is evident from Fig. 3 that in the shock-compressed gas charge the density values measured with and without inserts are similar. This indicates that the inserts do not introduce significant perturbations into the flow passing between them.

With passage along the tube, the turbulent mixing region not only increases in size, but, as is evident from Fig. 3, a change occurs in the driven gas density distribution. At a distance of  $15d$  from the diaphragm there is a marked falloff in driven gas density at the boundary between the hot charge and the contact region. At the beginning and end of the mixing zone the mean density measured in the presence of inserts was greater than the mean density measured without them. This indicated that at the edges of the mixing zone the mean density of the driven gas in the flow core is somewhat higher than at the walls. In the section B ( $X = 92d$ ) the driven gas density at the leading edge of the contact region is comparable to the density at the end of the hot charge, moreover, the values of  $\langle \rho \rangle$ , measured for two different values of  $h$ , differ only slightly. Hence we may conclude that the density distribution of the driven gas is relatively homogeneous across the tube at the beginning of the mixing zone with some increase in inhomogeneity toward the end of the zone. Since with decrease in  $h$  density fluctuations do not increase markedly, the size of inhomogeneities in the cross section is probably several times smaller than  $h$ , i.e., does not exceed 1 cm. Thus, as the

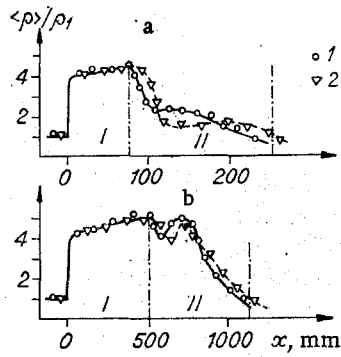


Fig. 3

shock wave propagates the density at the leading edge of the contact region decreases, and the boundary itself becomes more planar. The trailing edge of the mixing region preserves its convex form. The mean density of the driven gas changes nonmonotonically along the mixing region.

The driver gas density distribution was obtained in experiments in which the high pressure chamber was filled not with helium, but with a mixture of 98.8% H<sub>2</sub> + 1.2% Xe, which has a speed of sound close to the speed of sound in helium; the density distribution of the driven gas was assumed known from the previous series of experiments. Figure 4 shows the distribution of mean density of the driven 1 and driver (dash-dot curves) gases and the net density 2 in the hot charge, in the contact gas mixing region and in the driver gas flow behind the mixing region. Measurements showed that the pressure remains constant over the entire flow zone studied. The largest changes in densities of driver and driven gases are found at the leading boundary of the mixing region, and must be accompanied by an abrupt drop in temperature. The nonmonotonic distribution of total density in the mixing region should be noted. The dashed line of Fig. 4 shows the driver gas density distribution in an ideal charge. It is evident how much this value falls due to turbulent mixing of the gases. The calculation was performed for a Mach number M<sub>0</sub> = 9.

The ratio of the mass of gas in the contact mixing region to the mass of an ideal charge

$$m_{\text{cmr}} / m_0 = \int_{\text{II}} \langle \rho \rangle dx / \rho_0 X \quad (\rho_0 \text{ (where } \rho_0 \text{ is the initial density, } X \text{ is the distance from diaphragm to}$$

measurement section) at three shock tube sections (dark points) together with the increase in length of the contact region (light points) with motion along the shock tube for various regimes are shown in Fig. 5: 1) p<sub>0</sub> = 5.5 kPa, M<sub>0</sub> = 10; 2) p<sub>0</sub> = 1.7 kPa, M<sub>0</sub> = 9; 3) p<sub>0</sub> = 13.3 kPa, M<sub>0</sub> = 6. In the contact region 35 to 50% of the mass of an ideal charge is found. The length of the turbulent contact region increases approximately in proportion to the contact region to the distance traversed. As follows from Fig. 5, the increase in the contact region depends only weakly on experimental conditions. The increase in size of the gas mixing region indicates the instability of the leading boundary of the contact region. As it moves along, the shock wave compresses and draws new layers into the shock-compressed gas charge, and as a result of turbulent mixing on the boundary with the contact region a portion of the gas moves into the mixing region, which leads to growth of the latter. It should be noted that gas which is carried off from the hot charge through the boundary layer can diffuse into the core of this region. Mirels' theory [18] allows estimation of the gas flow rate through the boundary layer. In order to determine the accuracy of this theory, a special experiment was performed [19]. Apparently the Mirels theory produces an exaggerated (maximum) estimate of the role of the boundary layer. To determine the fractions of gas entering into the contact mixing region from the boundary layer further study will be required. In the present study we have only established that the driven and driver gases do mix.

The basic characteristics of the turbulent flow in the mixing zone can be estimated from the experimental data. For the regime p<sub>0</sub> = 1.7 kPa, m<sub>0</sub> = 9 the calculated flow velocity behind the shock wave front u<sub>c</sub> = 1.2 · 10<sup>5</sup> cm/sec. Assuming for the estimates that the contact region propagation velocity is constant and equal to the velocity of the companion flow, we will determine the expansion velocity v<sub>e</sub> of the turbulent zone. In the section X = 4.6 m the length of the mixing zone l<sub>cmr</sub> = 90 cm, then v<sub>e</sub> = l<sub>cmr</sub>u<sub>c</sub>/X = 2.4 · 10<sup>4</sup> cm/sec. The pulsation

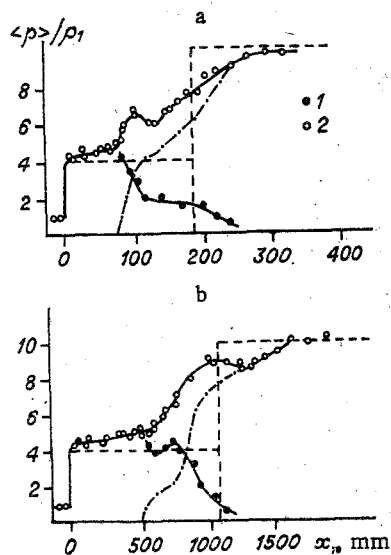


Fig. 4

velocity  $v'$  is usually comparable to the expansion velocity, and is apparently several times smaller than the flow velocity ( $v' = (2-3) \cdot 10^4$  cm/sec). The present experiments do not provide sufficient information to determine the mixing path length. The latter value can be estimated using the recommendation of [6]:  $l_{\text{mix}} \approx 0.1 l_{\text{cmr}} \approx 9$  cm. The turbulent diffusion coefficient is defined as  $D_T \approx v' l_{\text{mix}} \approx 2 \cdot 10^5$  cm/sec, an order of magnitude larger than the molecular diffusion coefficient. Since the turbulent zone expansion rate is practically constant, it may be concluded that the turbulent diffusion coefficient increases with time.

To establish the causes responsible for increase in the length of the mixing zone and increase in the amount of driven gas drawn into this zone, we must first clarify whether these are direct consequences of initial perturbations arising upon diaphragm rupture, or whether factors act far from the diaphragm, leading to instability of the contact surface and flow turbulization. The initial turbulence is created by rupture and escape of a jet of driver gas through the opening diaphragm. Moreover, as was shown in [10], a series of shock waves are generated in the diaphragm region. Relying on the results of [20] concerning interaction of shock waves with a turbulent contact surface, it can be proposed that these shock waves intensify turbulent mixing of the gases. It is evident that all these factors act until the process of diaphragm opening is completed. As follows from the results of [21], the diaphragms used in the present experiment open in a period of about 300  $\mu\text{sec}$ . Thus, in the first measurement section the contact region arrives after diaphragm opening is completed, while the time of arrival at the last measurement section is 15 times greater than the diaphragm opening time. The rate at which the initial turbulence degenerates can be considered using the example of degeneration of turbulence produced by acceleration of the boundary after acceleration terminates. Such a problem was considered theoretically in [6]. It develops that if the time after termination of acceleration is 2-4 times greater than the time over which acceleration acts, the turbulent zone continues to increase with time as  $l \sim t^{1/2}$ , or if the time after termination of acceleration is an order of magnitude larger than  $l \sim t^{1/4}$ . In experiment,  $l \sim t$ ; consequently the observed increase in length of the mixing region most probably occurs not as a consequence of inertia of the initial turbulence, but due to activation of some additional mechanisms.

In a real shock tube the flow velocity at the end of the charge of shock-compressed gas at the boundary with the contact region can change with motion along the shock tube. Available data on shock wave front retardation with motion along the channel and on increase in velocity of the companion flow with time at a fixed section do not permit an unambiguous conclusion as to the change with time of gas velocity on the boundary. Data are available on the propagation rate of the forward boundary of the turbulent region, obtained by timed shadow photography at various distances from the diaphragm [1]. Toward the end of the tube this velocity has increased by 30-40%, which was interpreted as an acceleration of the contact region front. However it is obvious that this velocity is a combination of the propagation velocity of the gas flow and the propagation velocity of the gas along the forward boundary of the mixing region, so that the results of this and similar studies cannot provide information on the flow velocity on the boundary. Thus, the question of gas acceleration on the boundary with the contact

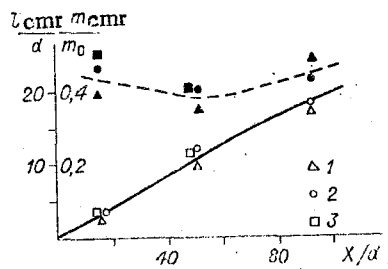


Fig. 5

region remains open. If such acceleration is opposite to the pressure gradient, then Rayleigh-Taylor instability will develop on the boundary. As experiment has shown, the gas density in the contact region changes nonmonotonically. In the center of the region  $\partial \langle \rho \rangle / \partial x < 0$ , and upon flow acceleration conditions exist for development of instability. Near the forward boundary of the region  $\partial \langle \rho \rangle / \partial x > 0$ , and instability can develop in the case of flow retardation. From analysis of all concepts of shock tube operation [1, 17] it can be concluded that far from the diaphragm there is no marked retardation (2% at 1 m length in the low pressure chamber), while the possible acceleration does not exceed 10% at 1 m length of the low pressure chamber. It will be useful to evaluate the length of the turbulent region in the simplest possible case where we assume that the initial density boundaries are planar, the flow is unperturbed, and the flow acceleration is equal to the hypothetical acceleration. For approximate calculations we may use the isothermal approximation [6]. We will estimate the length of the turbulent region upon development of Rayleigh-Taylor instability for two cases: flow retardation (instability develops on the forward edge of the contact region) and flow acceleration (instability may develop in the middle of the contact region). It develops that in either variant the calculated length of the turbulent region in the last measurement section does not exceed 2 cm, i.e., is significantly less than that observed experimentally. This allows the assumption that if the boundary between the gases is turbulized initially, further turbulization with flow acceleration occurs more rapidly than in the case of an initially unperturbed boundary.

The development of the turbulent region has a significant effect on the characteristics of the shock-compressed gas charge. It leads to reduction in size of the hot charge [3, 15] and can affect measurement results, leading to scattering under conditions where the length of the hot charge is comparable to the tube diameter or when measurements are performed at the end of the charge. Material on the radiating ability of argon measured in various shock tubes was presented in [22], with a detailed analysis of causes leading to the observed scattering of experimental data. It is apparent that the mechanism presented above should be added to the number of possible causes. Moreover, instability of the forward edge of the turbulent region may lead to the excitation of oscillations in the hot charge.

It has thus been demonstrated that the turbulent mixing zone formed upon diaphragm rupture increases in size with propagation along the channel far from the diaphragm. The densities of driven and driver gases have been measured in the mixing zone, and a nonmonotonic density distribution along the mixing zone has been observed. The expansion rate of the turbulent region has been estimated. Possible mechanisms leading to an increase in the length of the turbulent zone and the mass of driven gas drawn into the zone have been evaluated. It has been demonstrated that the new data obtained on shock tube operation permit a more correct interpretation of experimental results.

#### LITERATURE CITED

1. Kh. A. Rakhmatullin and S. S. Semenov (eds.), Shock Tubes [Russian translation], IL, Moscow (1962).
2. E. V. Stupochenko, S. A. Losev, and A. I. Isopov, Relaxation Processes in Shock Tubes [in Russian], Nauka, Moscow (1965).
3. R. V. Vasil'eva, A. D. Zuev, and D. N. Mirshanov, "Driven gas distribution in a shock tube and charge structure behind strong shock waves," Zh. Tekh. Fiz., 49, No. 2 (1979).
4. M. A. Levine, "Turbulent mixing at contact surface in a driven shock wave," Phys. Fluids, 13, No. 5 (1970).
5. A. N. Davydov, E. F. Lebedev, and S. A. Perkov, "Experimental study of gas dynamic instability in a plasma flow behind a cylindrical shock wave," Preprint IVTAN 1246 (1979).

6. S. Z. Belen'kii and E. S. Fradkin, "Turbulent mixing theory," Tr. FIAN, 29, 207 (1965).
7. V. E. Neuvazhaev and V. G. Yakovlev, "Turbulent mixing of the boundary in numerical gas dynamic calculation," Zh. Vychisl. Mat. Mat. Fiz., 16, No. 2 (1976).
8. D. R. White, "Influence of diaphragm opening time on shock flows," J. Fluid Mech., 4, No. 6 (1958).
9. V. T. Kireev, "Shock wave motion with noninstantaneous diaphragm opening in a shock tube," Izv. Akad. Nauk SSSR, Mekh. Mashinostr., 7, No. 2 (1962).
10. L. S. Shtemenko, "Gas flow near a diaphragm in a shock tube," Vestn. Mosk. Gos. Univ., Fiz. Astronom., No. 1 (1967).
11. L. S. Shtemenko, "Development of a density discontinuity in the initial period of gas flow near a diaphragm in a shock tube," Vestn. Mosk. Gos. Univ., Fiz. Astronom., No. 3 (1968).
12. T. Ikui, K. Matsuo, and N. Nagai, "Investigation of the aerodynamic characteristics of shock tubes," Bull. Jpn. Soc. Mech. Eng., 12, No. 52 (1969).
13. A. M. Naumov and R. Ya. Tugazakov, "Calculation of flows in a shock tube near an opening diaphragm," Uchen. Zap. TsAGI, 7, No. 2 (1976).
14. W. Hooker, "Testing time and contact-zone phenomena in shock tube flow," Phys. Fluids, 4, No. 12 (1961).
15. A. D. Zuev and D. N. Mirshanov, "Use of x-ray diagnostics for study of a charge of shock-compressed gas and the contact mixing region," Teplofiz. Vys. Temp., 19, No. 5 (1981).
16. R. V. Vasil'eva, "Measurement of the velocity of the companion gas flow in a shock tube by induced emf," Zh. Prikl. Mekh. Tekh. Fiz., No. 5 (1965).
17. T. V. Bazhenova and L. G. Gvozdeva, Nonsteady State Shock Wave Interactions [in Russian], Nauka, Moscow (1977).
18. H. Mirels, "Boundary layer effect in shock tubes," in: Shock Tube Research, London (1971).
19. A. D. Zuev, "The effect of the boundary layer on flow parameters in a shock tube," Preprint FTI Akad. Nauk SSSR, No. 714 (1981).
20. V. A. Andronov, S. M. Bakhrakh, et al., "Turbulent mixing on a contact surface accelerated by shock waves," Zh. Eksp. Teor. Fiz., 71, No. 2 (8) (1976).
21. E. M. Rothkopf and W. Low, "Diaphragm opening process in shock tubes," Phys. Fluids, 17, No. 6 (1974).
22. B. K. Tkachenko, "Unique features of high temperature flows in shock tubes and scattering of experimental data," in: Materials of the International Seminar-School "High Temperature Gas Dynamics, Shock Tubes, and Shock Waves" [in Russian], Minsk (1983).